

Supplementary Information

Effect of Polysiloxane Encapsulation Material Compositions on Emission Behaviour and Stabilities of Perylene Dyes

Nils Steinbrück^a, Martin Könemann^b and Guido Kickelbick^c

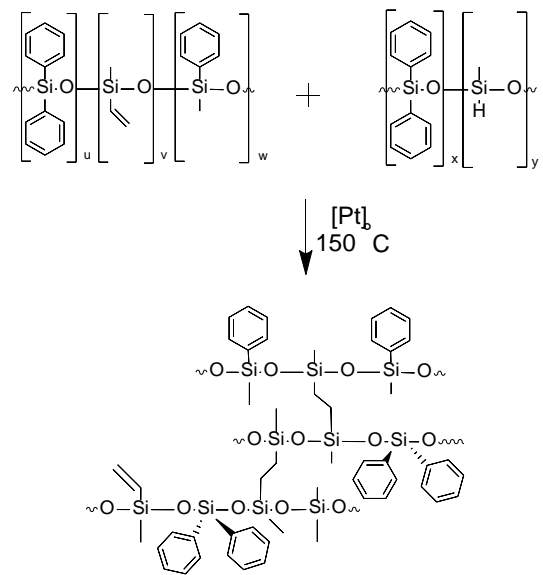
^aSaarland University, Inorganic Solid State Chemistry, Campus, Building C4 1, 66123 Saarbrücken, Germany.

^bBASF SE, 67056 Ludwigshafen, Germany

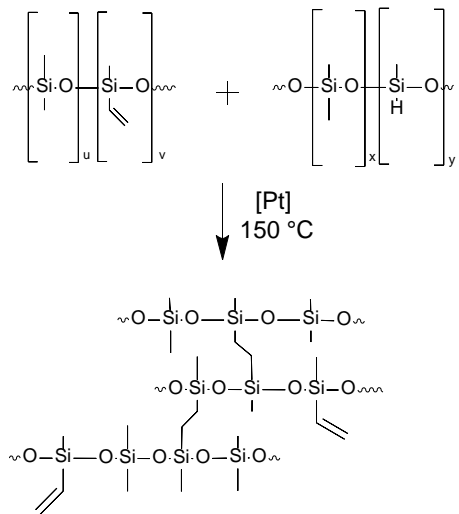
E-mail: guido.kickelbick@uni-saarland.de

Reaction schemes of Dow(1) and Shin(1) curing process.....	3
Synthesis of FC546	4
Preparation of N,N'-diallyl-1,6,7,12-tetrachloroperylene-3,4,9,10-tetracarboxylic acid diimide (I)	4
Preparation of N,N'-diallyl-2,4,4-trimethylpentan-2-yl phenoxy-3,4,9,10-tetracarboxylic acid diimide (II) [FC546].....	4
IR-Spectroscopy	5
NMR-Spectroscopy	11
Quantum yield and SA-Coefficient.....	13
Bleaching UV-VIS (Air)	25
Bleaching UV-VIS (Nitrogen/Air).....	27
Verification of covalent bond formation between a Si-H containing polymer and FC546	31

Reaction schemes of Dow(1) and Shin(1) curing process



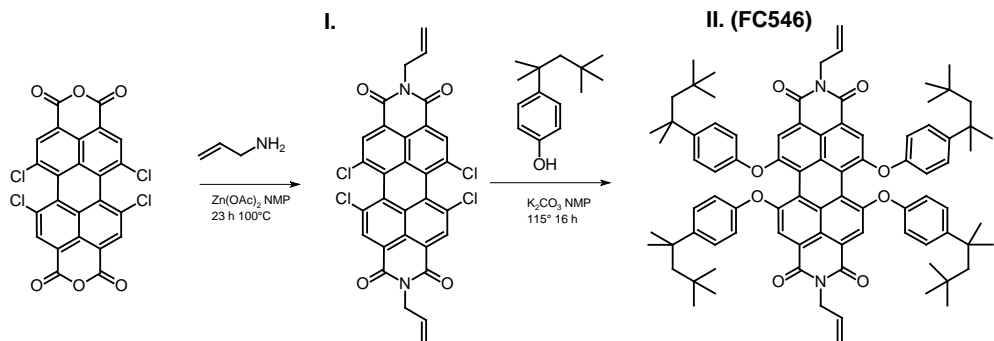
Scheme 1. Schematic chemical equation for the platinum catalysed hydrosilylation curing process of Dow(1).



Scheme 2. Schematic chemical equation for the platinum catalysed hydrosilylation curing process of Shin(1).

Synthesis of FC546

FC546 was synthesized by BASF SE in a two-step procedure.



Scheme 3. Two step synthesis of FC546.

Preparation of N,N'-diallyl-1,6,7,12-tetrachloroperylene-3,4,9,10-tetracarboxylic acid diimide (I)

A mixture of 2.65 g (5 mmol) of 1,6,7,12-tetrachloroperylene-3,4;9,10-tetracarboxylic acid dianhydride, 2.75 g (15 mmol) of zinc acetate, 30 mL of N-methylpyrrolidone and 1.52 g (26 mmol) of allylamine were heated to 100°C for 23 hours. The reaction mixture was cooled to room temperature and 250 mL of brine were added. The formed solid was isolated by filtration, washed with water and dried at 70°C under reduced pressure. The product was used without further purification for the next step.

R_f (toluene:acetone 100:1) = 0.45.

Preparation of N,N'-diallyl-2,4,4-trimethylpentan-2-yl phenoxy-3,4,9,10-tetracarboxylic acid diimide (II) [FC546]

A mixture of 3.04 g (5 mmol) of the compound I, 70 mL of N-methylpyrrolidone, 5.16 g (25 mmol) of tert.-octylphenol, 3.46 g (25 mmol) of potassium carbonate was heated for 21 hours to 115°C . The reaction mixture was cooled to room temperature, the solid was isolated by filtration, the residue washed with water and dried at 70°C under reduced pressure. The product was subjected to column chromatography using toluene petroleum ether 1:2 and 1:1 and toluene. 1.2 g (19 %) of pure product were isolated.

R_f (toluene) = 0.36.

^1H NMR spectrum and chemical shifts are shown in the NMR section.

IR-Spectroscopy

Dow Corning OE6630 component A (cm^{-1}): 3049, 3072 $\nu(\text{C-H})_{\text{AR}}$; 2953, 2909 $\nu(\text{C-H})$; 1590, 1490, 1430 [$\nu(\text{C=C-C})_{\text{AR}}$]; 1413, 1257 [$\delta(\text{C-H}[\text{Si-CH}_3])$]; 1115, 1024 [$\nu(\text{Si-O-Si})$]; 784 [$\rho(\text{C-H}[\text{Si-(CH}_3)_2])$]; 726, 694 [$\delta(\text{C-H})_{\text{AR}}$].

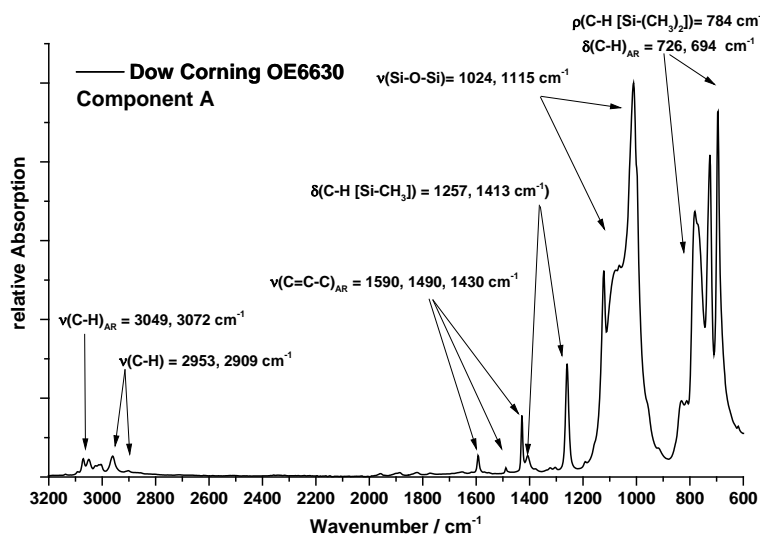


Figure 1. FTIR spectrum of Dow Corning OE6630 component A.

Dow Corning OE6630 component B (cm^{-1}): 3049, 3072 $\nu(\text{C-H})_{\text{AR}}$; 2953, 2909 $\nu(\text{C-H})$; 2129 [$\nu(\text{Si-H})$]; 1590, 1490, 1430 [$\nu(\text{C=C-C})_{\text{AR}}$]; 1413, 1257 [$\delta(\text{C-H}[\text{Si-CH}_3])$]; 1115, 1024 [$\nu(\text{Si-O-Si})$]; 896 [$\rho(\text{Si-H})$]; 784 [$\rho(\text{C-H}[\text{Si-(CH}_3)_2])$]; 726, 694 [$\delta(\text{C-H})_{\text{AR}}$].

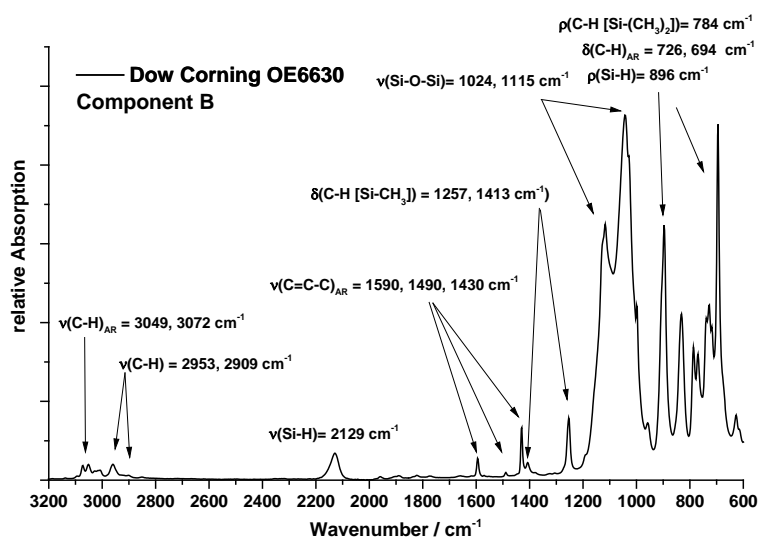


Figure 2. FTIR spectrum of Dow Corning OE6630 component B.

Shin KJR9022E component A (cm^{-1}): 2960, 2902 $\nu(\text{C-H})$; 1412, 1257 [$\delta(\text{C-H}[\text{Si-CH}_3])$]; 1008, 1065 [$\nu(\text{Si-O-Si})$]; 784 [$\rho(\text{C-H}[\text{Si-(CH}_3]_2)]$].

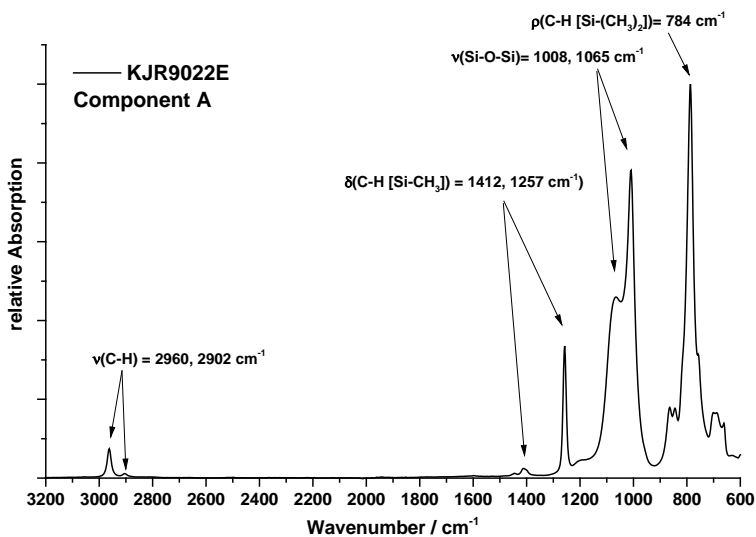


Figure 3. FTIR spectrum of Shin Etsu KJR9022E component A.

Shin KJR9022E component B (cm^{-1}): 2960, 2902 $\nu(\text{C-H})$; 2159 [$\nu(\text{Si-H})$]; 1412, 1257 [$\delta(\text{C-H}[\text{Si-CH}_3])$]; 1008, 1065 [$\nu(\text{Si-O-Si})$]; 906 [$\rho(\text{Si-H})$]; 784 [$\rho(\text{C-H}[\text{Si-(CH}_3]_2)]$].

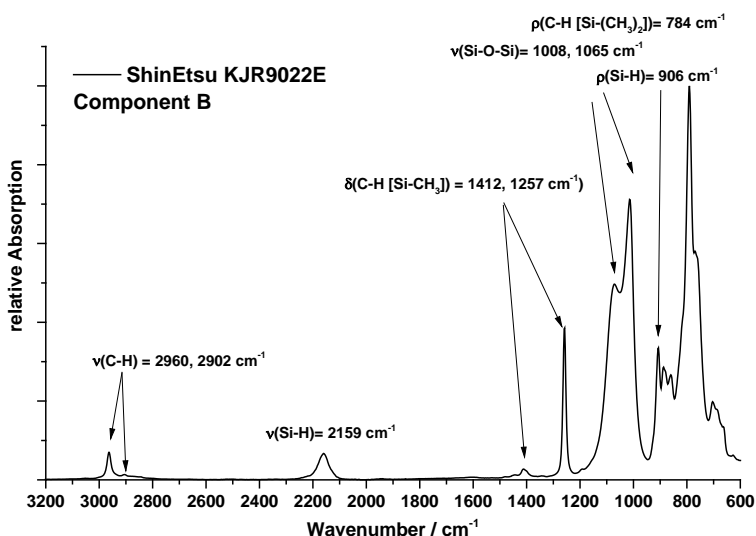


Figure 4. FTIR spectrum of Shin Etsu KJR9022E component B.

Dow Corning OE6630 cured (cm^{-1}): 3049, 3072 $\nu(\text{C-H})_{\text{AR}}$; 2953, 2909 $\nu(\text{C-H})$; 1590, 1490, 1430 [$\nu(\text{C=C-C})_{\text{AR}}$]; 1413, 1257 [$\delta(\text{C-H [Si-CH}_3)]$]; 1115, 1024 [$\nu(\text{Si-O-Si})$]; 784 [$\rho(\text{C-H [Si-(CH}_3]_2)]$]; 726, 694 [$\delta(\text{C-H})_{\text{AR}}$].

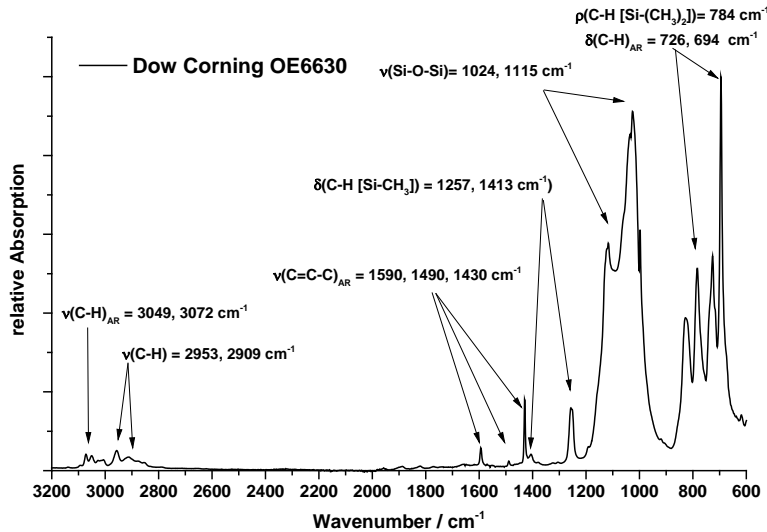


Figure 5. FTIR spectrum of cured Dow Corning OE6630.

Shin KJR9022E cured (cm^{-1}): 2960, 2902 $\nu(\text{C-H})$; 1412, 1257 [$\delta(\text{C-H [Si-CH}_3)]$]; 1008, 1065 [$\nu(\text{Si-O-Si})$]; 784 [$\rho(\text{C-H [Si-(CH}_3]_2)]$].

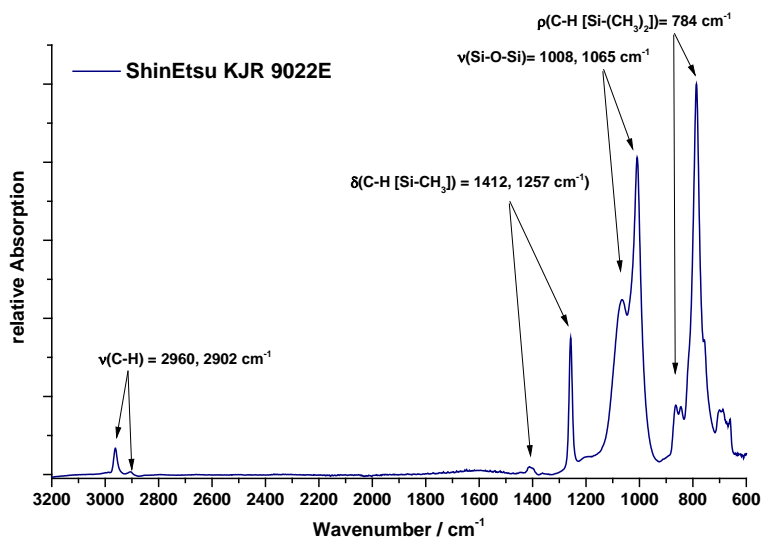


Figure 6. FTIR spectrum of cured ShinEtsu KJR9022E.

Lumogen®F Red 305 (cm^{-1}): 3030, 3064 $\nu(\text{C-H})_{\text{AR}}$; 2960, 2925 $\nu(\text{C-H})$; 1705, 1672 $\nu(\text{C=O})$; 1583, 1485 [$\nu(\text{C=C-C})_{\text{AR}}$]; 1407, 1338 $\nu(\text{C-N})$; 1309, 1282, 1193 $\nu(\text{C-O-C})$.

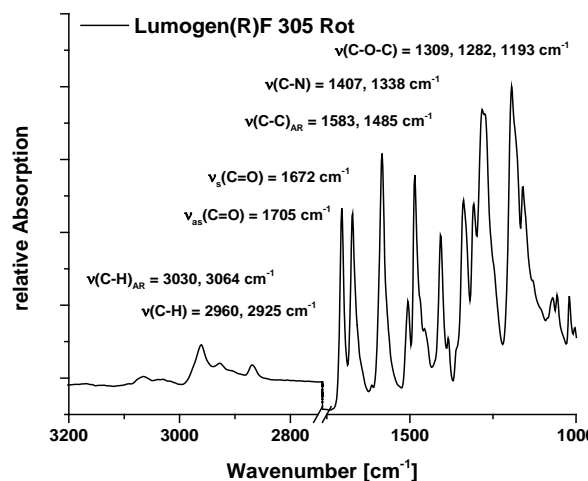


Figure 7. FTIR spectrum of Lumogen®F 305 Red.

FC546 (cm^{-1}): 3037, 3064 $\nu(\text{C-H})_{\text{AR}}$; 2920, $\nu(\text{C-H})$; 1699, 1662 $\nu(\text{C=O})$; 1585, 1502 [$\nu(\text{C=C-C})_{\text{AR}}$]; 1407, 1344 $\nu(\text{C-N})$; 1303, 1282, 1172 $\nu(\text{C-O-C})$.

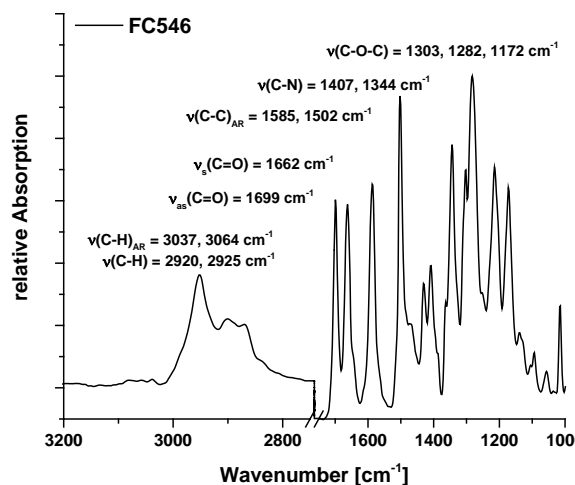


Figure 8. FTIR spectrum of FC546.

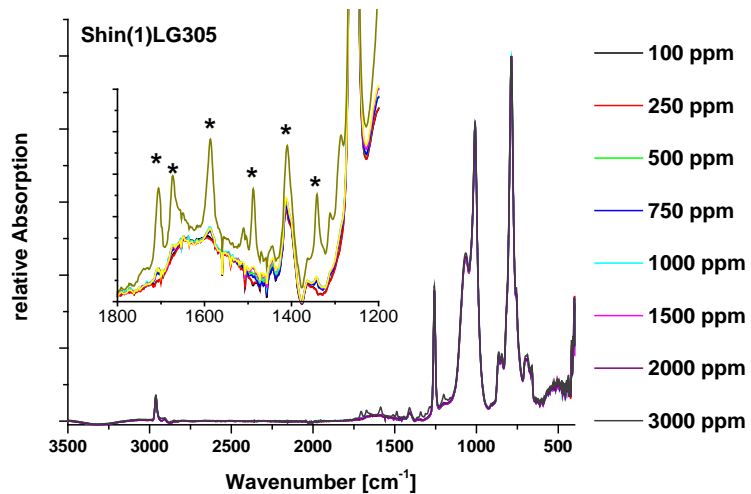


Figure 9. FTIR spectrum of Shin(1)LG305 concentration series.

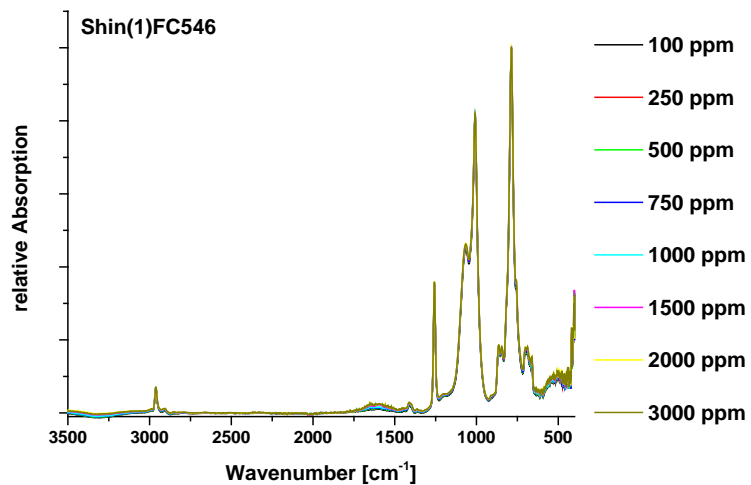


Figure 10. FTIR spectrum of Shin(1)FC546 concentration series.

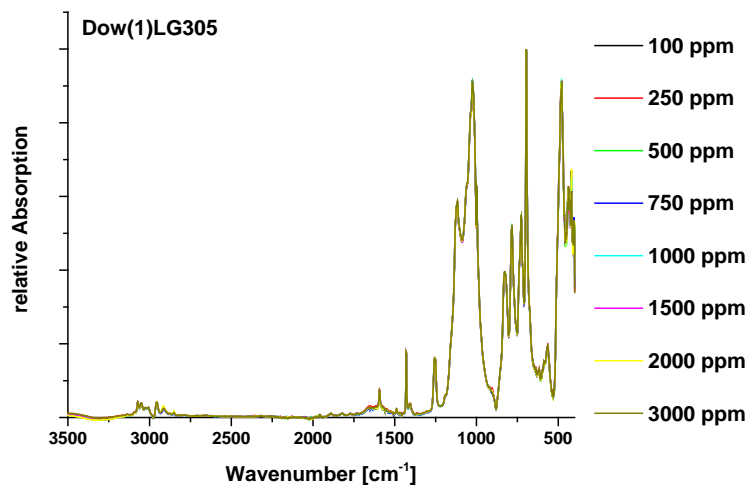


Figure 11. FTIR spectrum of Dow(1)LG305 concentration series.

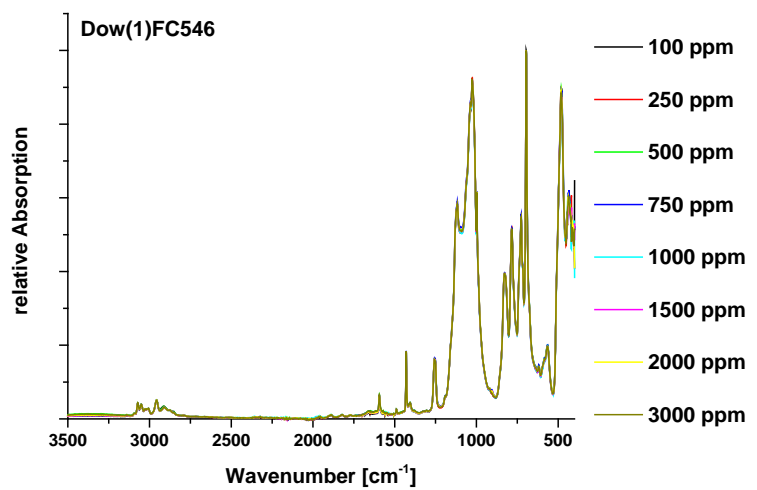
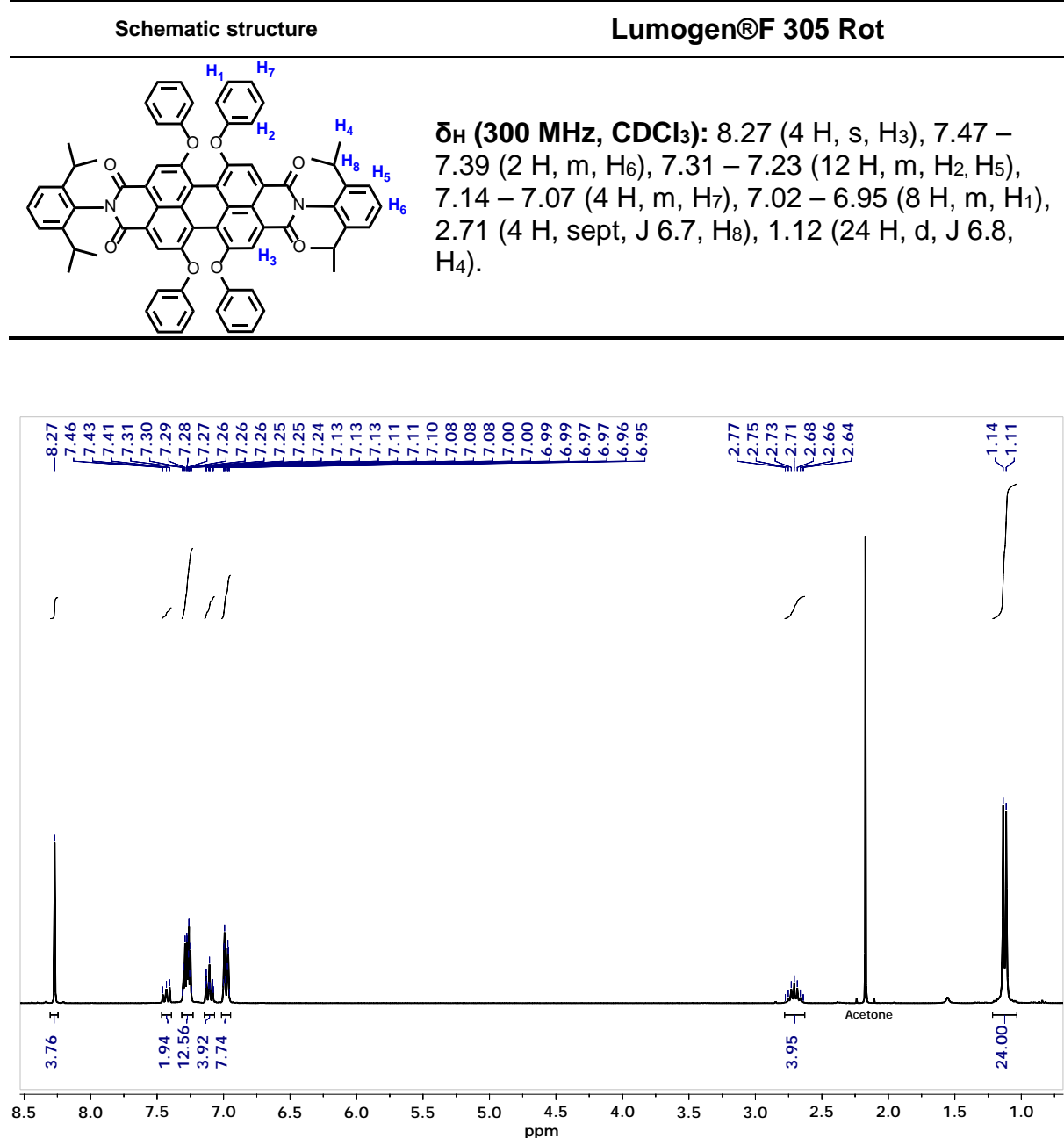
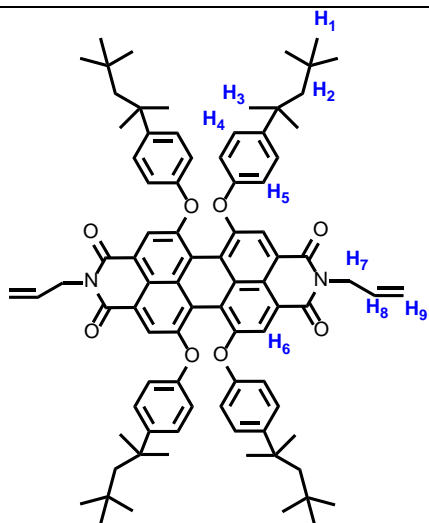


Figure 12. FTIR spectrum of Dow(1)FC546 concentration series.

NMR-Spectroscopy



Schematic structure**FC546**



δ_{H} (300 MHz, CDCl₃): 8.15 (4 H, s, H₆), 7.27 (8 H, d, J 6.9, H₄), 6.86 (8 H, d, J 8.0, H₅), 6.01 – 5.83 (2 H, m, H₈), 5.33 – 5.10 (4 H, m, H₉), 4.73 (4 H, d, J 5.3, H₇), 1.73 (8 H, s, H₂), 1.54 (s, water), 1.36 (24 H, s, H₃), 0.78 (36 H, s, H₁).

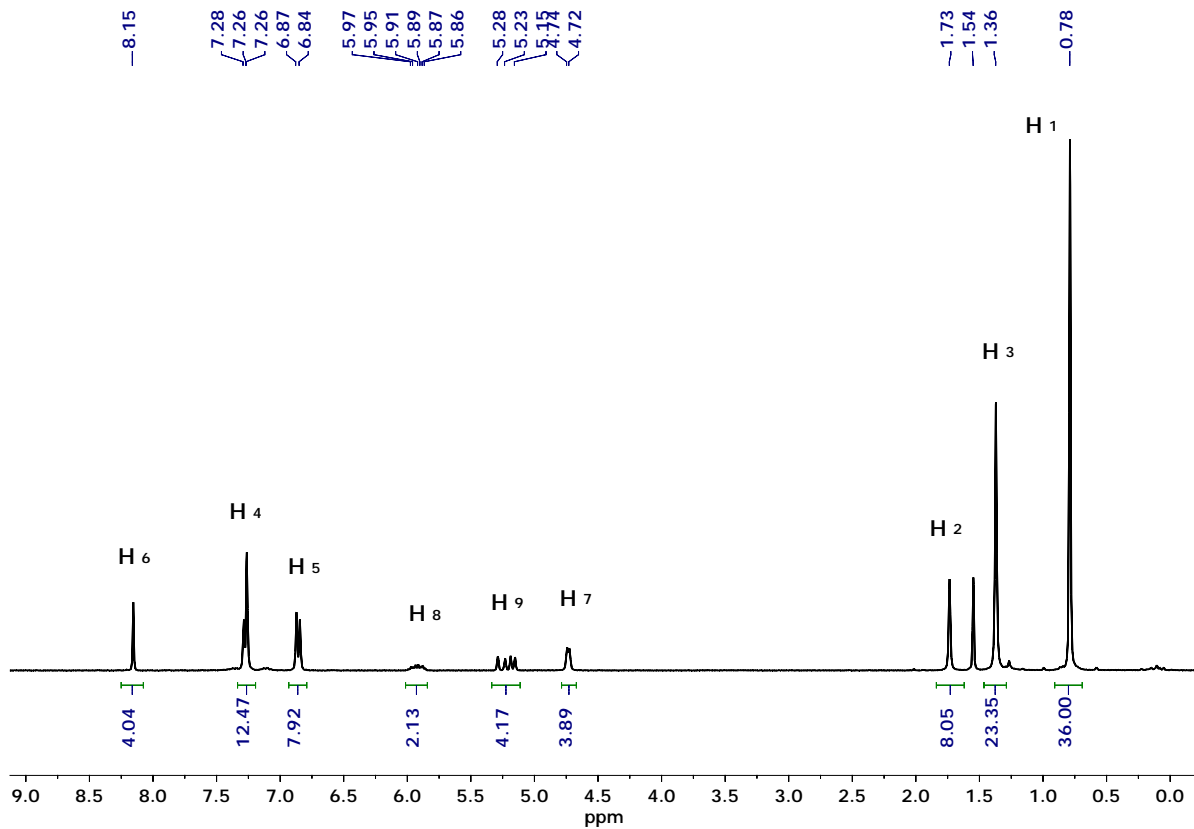


Figure 14. ¹H NMR spectrum of FC546.

Quantum yield and SA-Coefficient

Dow(1)LG305

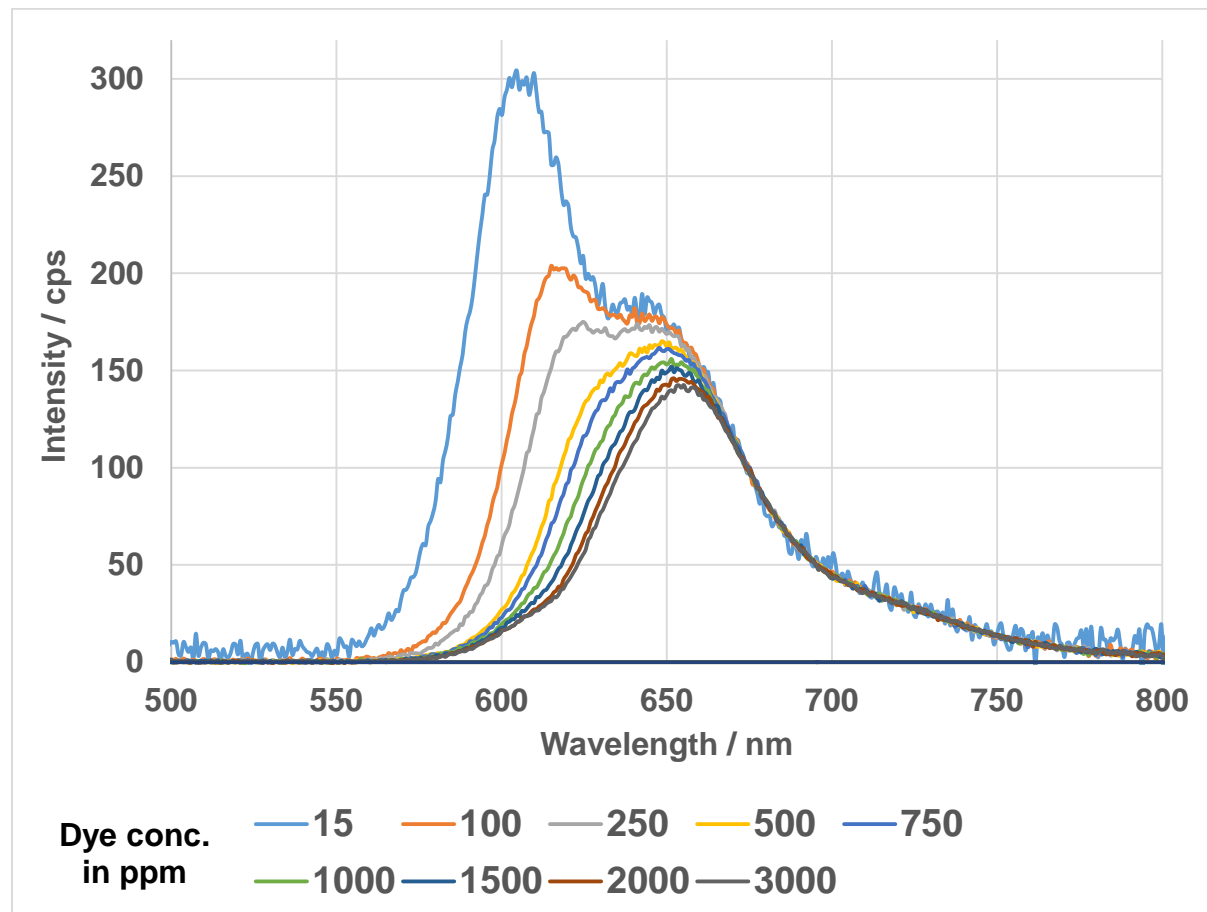


Figure 15. Fitted emission spectra of the Dow(1)LG305 concentration series quantum yield measurement and for the quantum yield correction and self-absorption coefficient calculations.

Table 1. Measured quantum yield values and calculated values of Dow(1)LG305 concentration series corrected quantum yield and the self-absorption coefficient. Goodness of the fit is calculated and given by the pearsons chi-squared test value χ^2 .

c / ppm	QE	QEcorr	a	χ^2
100	1,03	1,02	0,27	49,22
250	1,02	1,02	0,35	49,91
500	1,02	1,01	0,44	50,57
750	1,02	1,01	0,47	49,71
1000	1,00	1,00	0,50	49,91
1500	1,00	1,00	0,52	54,03
2000	1,00	1,00	0,55	53,21
3000	0,98	0,99	0,56	53,23

Dow(1)LG305 48h, 200 °C

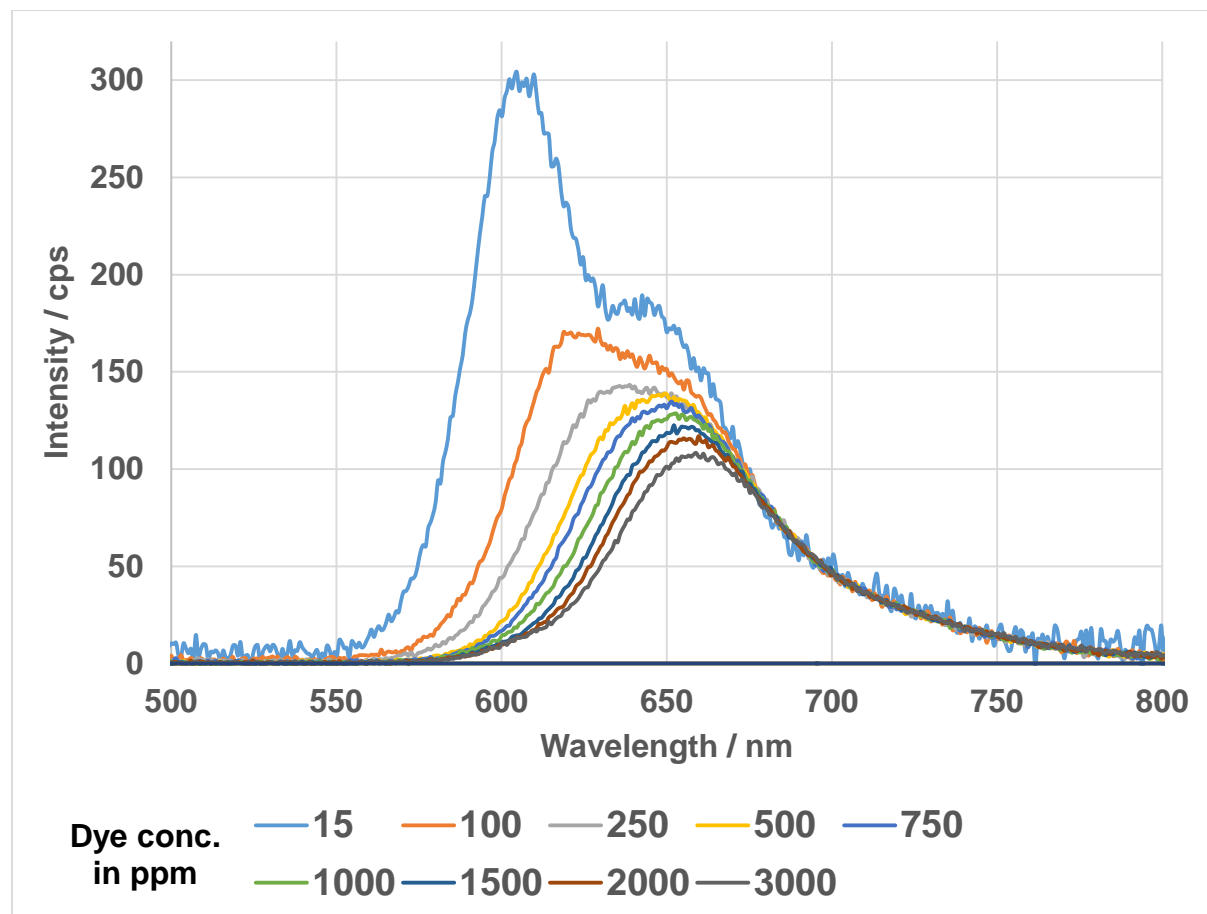


Figure 16. Fitted emission spectra of the Dow(1)LG305 48 h, 200 °C concentration series quantum yield measurement and for the quantum yield correction and self-absorption coefficient calculations.

Table 2. Measured quantum yield values and calculated values of the Dow(1)LG305 48 h, 200 °C concentration series corrected quantum yield and the self-absorption coefficient. Goodness of the fit is calculated and given by the pearsons chi-squared test value χ^2 .

c / ppm	QE	QEcorr	a	χ^2
100	0,91	0,94	0,34	65,46
250	0,93	0,96	0,45	62,54
500	0,92	0,96	0,51	56,28
750	0,91	0,96	0,54	55,58
1000	0,89	0,95	0,57	54,23
1500	0,88	0,95	0,59	54,43
2000	0,87	0,95	0,61	55,07
3000	0,85	0,94	0,64	54,94

Dow(1)LG305 120 h, 200 °C

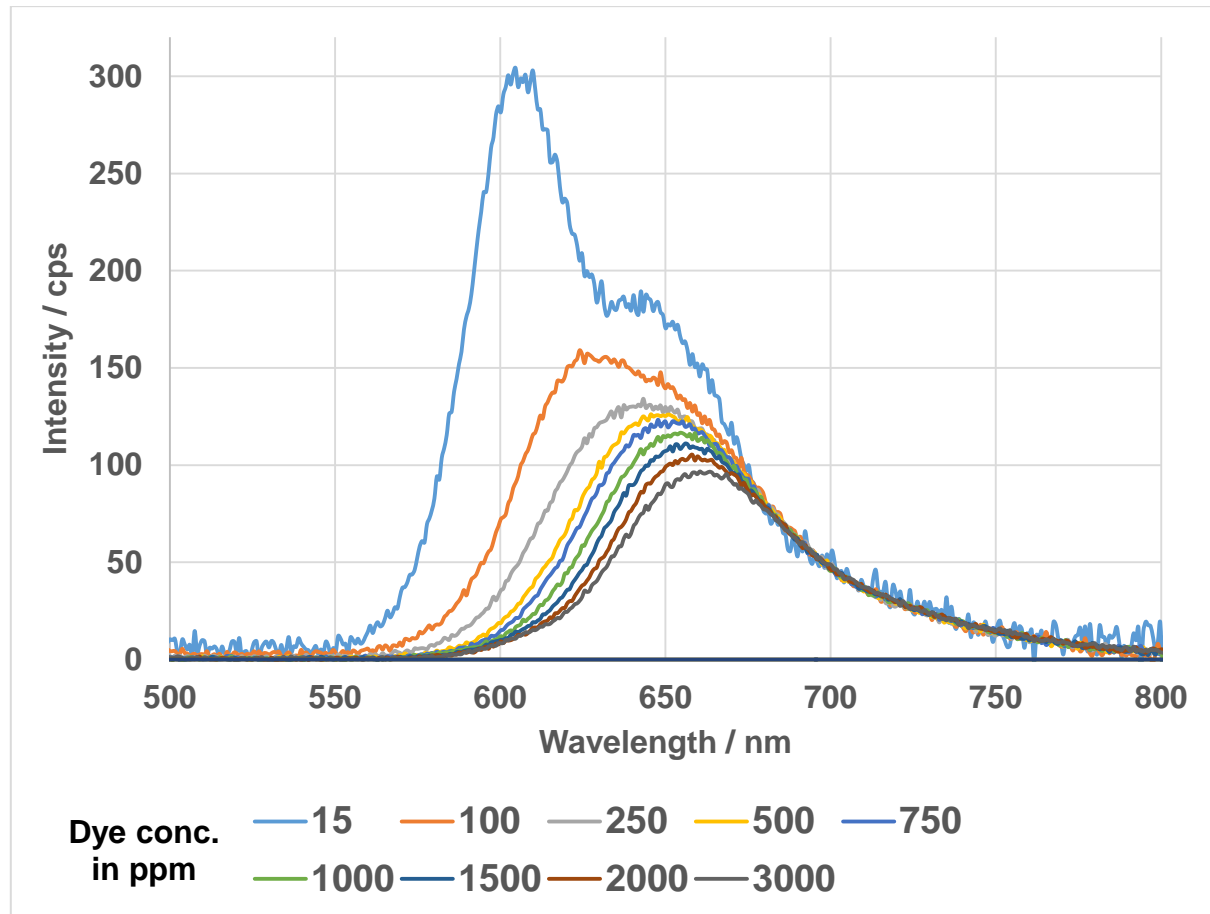


Figure 17. Fitted emission spectra of the Dow(1)LG305 120 h, 200 °C concentration series quantum yield measurement and for the quantum yield correction and self-absorption coefficient calculations.

Table 3. Measured quantum yield values and calculated values of the Dow(1)LG305 120 h, 200 °C concentration series corrected quantum yield and the self-absorption coefficient. Goodness of the fit is calculated and given by the pearsons chi-squared test value χ^2 .

c / ppm	QE	QEcorr	a	χ^2
100	0,86	0,91	0,38	58,36
250	0,87	0,93	0,49	63,29
500	0,87	0,93	0,54	58,14
750	0,87	0,94	0,56	57,49
1000	0,84	0,93	0,59	50,45
1500	0,83	0,93	0,62	50,90
2000	0,80	0,92	0,64	49,15
3000	0,78	0,91	0,66	57,38

Dow(1)FC546

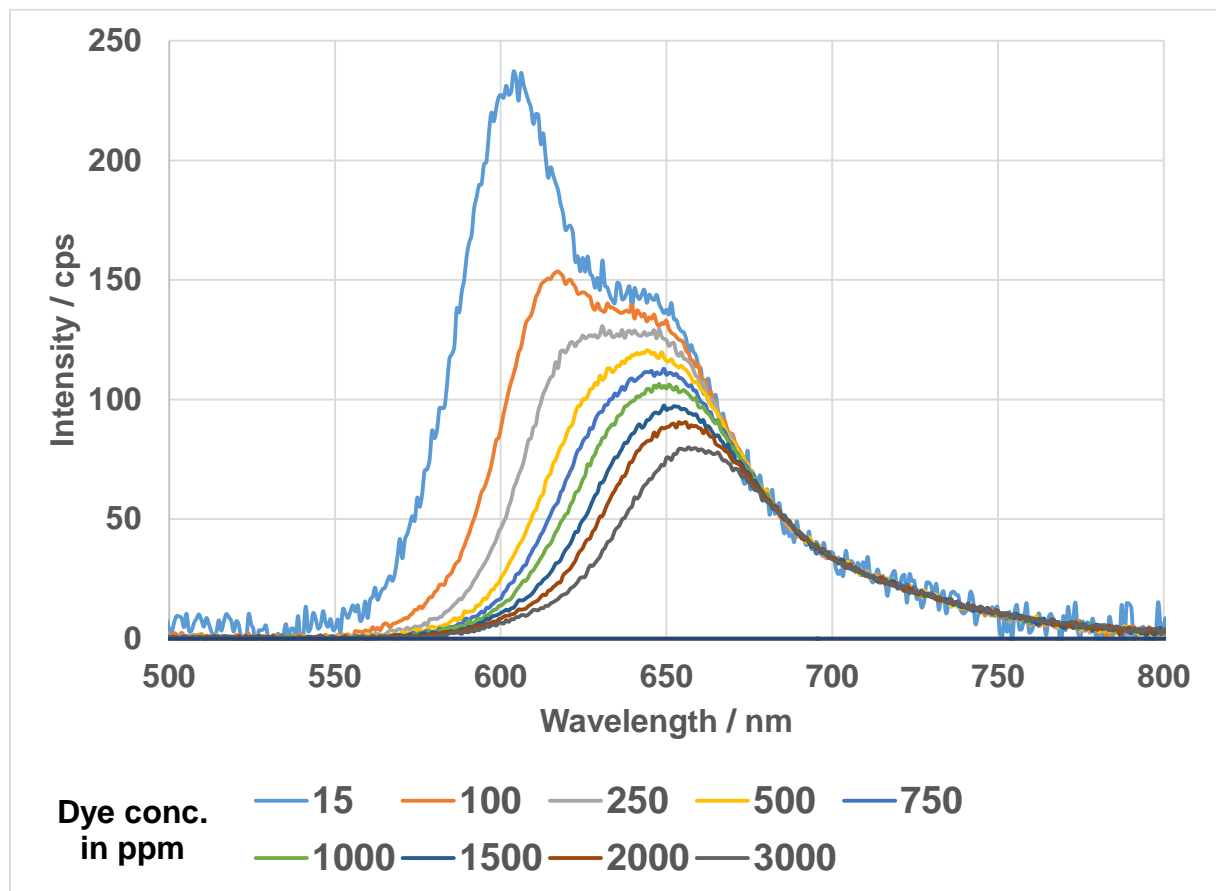


Figure 18. Fitted emission spectra of the Dow(1)FC546 concentration series quantum yield measurement and for the quantum yield correction and self-absorption coefficient calculations.

Table 4. Measured quantum yield values and calculated values of the Dow(1)FC546 concentration series quantum yield and the self-absorption coefficient. Goodness of the fit is calculated and given by the pearsons chi-squared test value χ^2 .

c / ppm	QE	QEcorr	a	χ^2
100	0,93	0,95	0,28	47,73
250	0,97	0,98	0,38	52,63
500	0,94	0,97	0,46	48,65
750	0,93	0,96	0,51	49,80
1000	0,91	0,96	0,54	51,59
1500	0,85	0,93	0,59	52,41
2000	0,82	0,92	0,62	50,74
3000	0,77	0,91	0,66	50,89

Dow(1)FC546 48 h, 200 °C

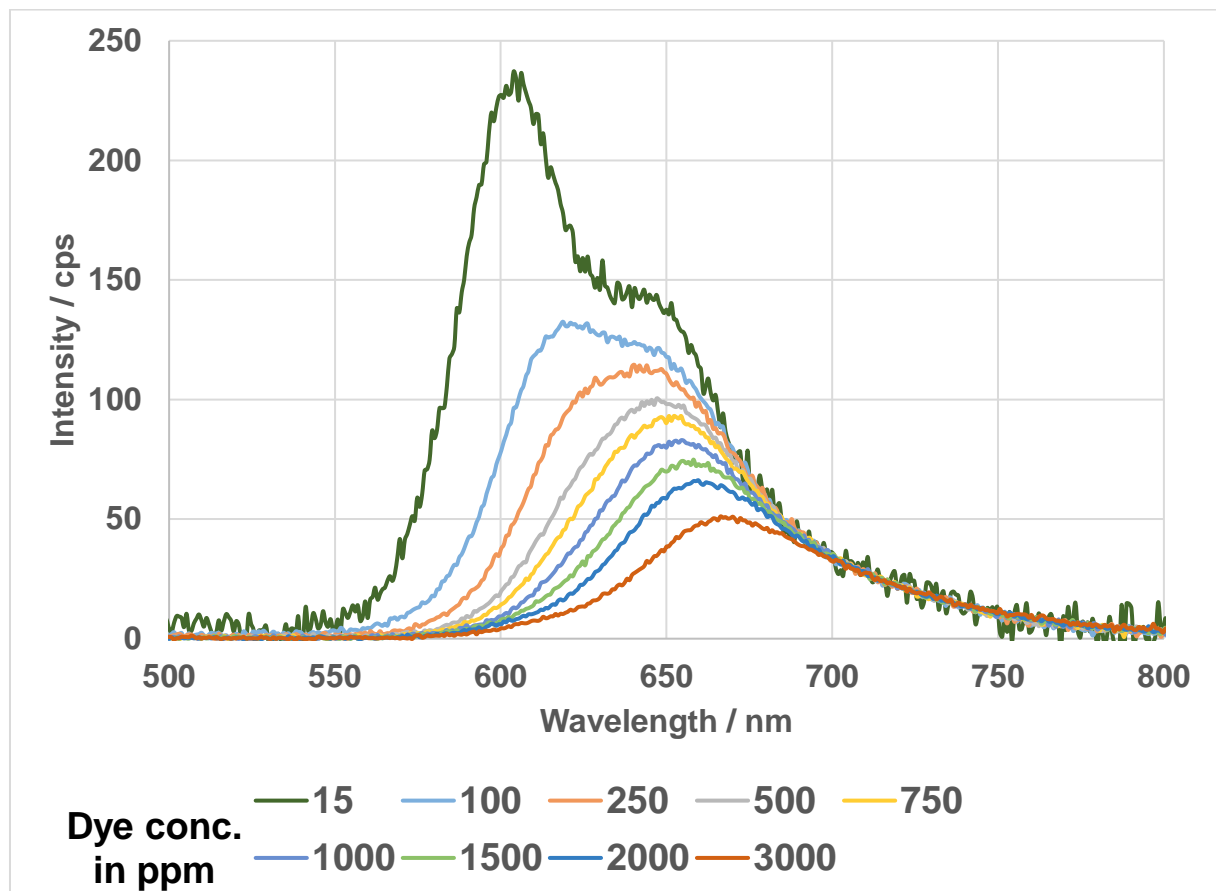


Figure 19. Fitted emission spectra of Dow(1)FC546 48 h, 200 °C concentration series quantum yield measurement and for the quantum yield correction and self-absorption coefficient calculations.

Table 5. Measured quantum yield values and calculated values of Dow(1)FC546 48 h, 200 °C concentration series corrected quantum yield and the self-absorption coefficient. Goodness of the fit is calculated and given by the pearsons chi-squared test value χ^2 .

c / ppm	QE	QEcorr	a	c2
100	0,87	0,91	0,33	51,79
250	0,88	0,93	0,45	54,55
500	0,84	0,92	0,54	48,00
750	0,81	0,91	0,58	51,40
1000	0,77	0,90	0,62	51,82
1500	0,72	0,88	0,66	51,56
2000	0,68	0,87	0,70	51,04
3000	0,58	0,84	0,75	49,79

Dow(1)FC546 120 h, 200 °C

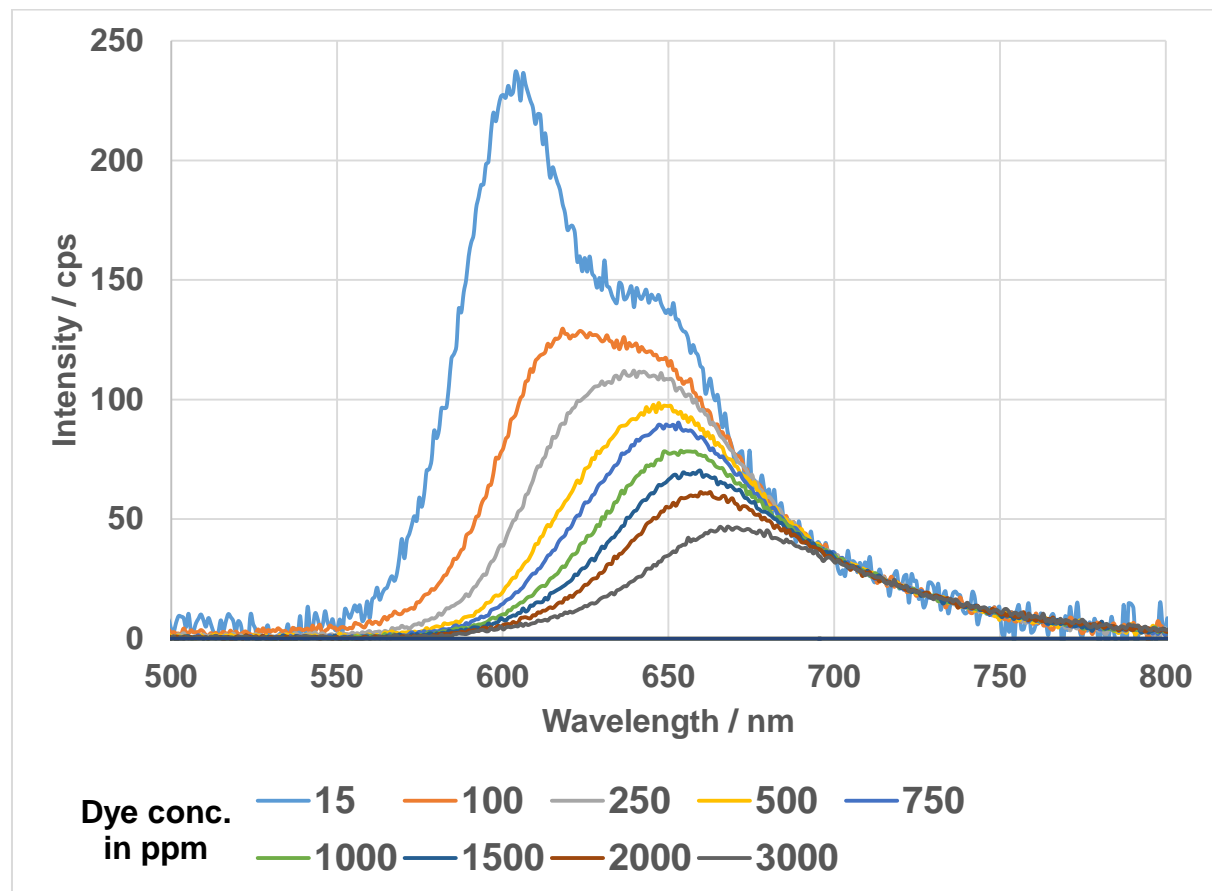


Figure 20. Fitted emission spectra of the Dow(1)FC546 120 h, 200 °C concentration series quantum yield measurement and for the quantum yield correction and self-absorption coefficient calculations.

Table 6. Measured quantum yield values and calculated values of the Dow(1)FC546 120 h, 200 °C concentration series corrected quantum yield and the self-absorption coefficient. Goodness of the fit is calculated and given by the pearsons chi-squared test value χ^2 .

c / ppm	QE	QEcorr	a	χ^2
100	0,86	0,90	0,33	52,17
250	0,82	0,89	0,45	50,89
500	0,78	0,89	0,54	52,31
750	0,79	0,90	0,59	51,58
1000	0,73	0,88	0,63	49,74
1500	0,69	0,87	0,67	51,69
2000	0,63	0,85	0,71	55,59
3000	0,53	0,83	0,76	52,50

Shin(1)FC546

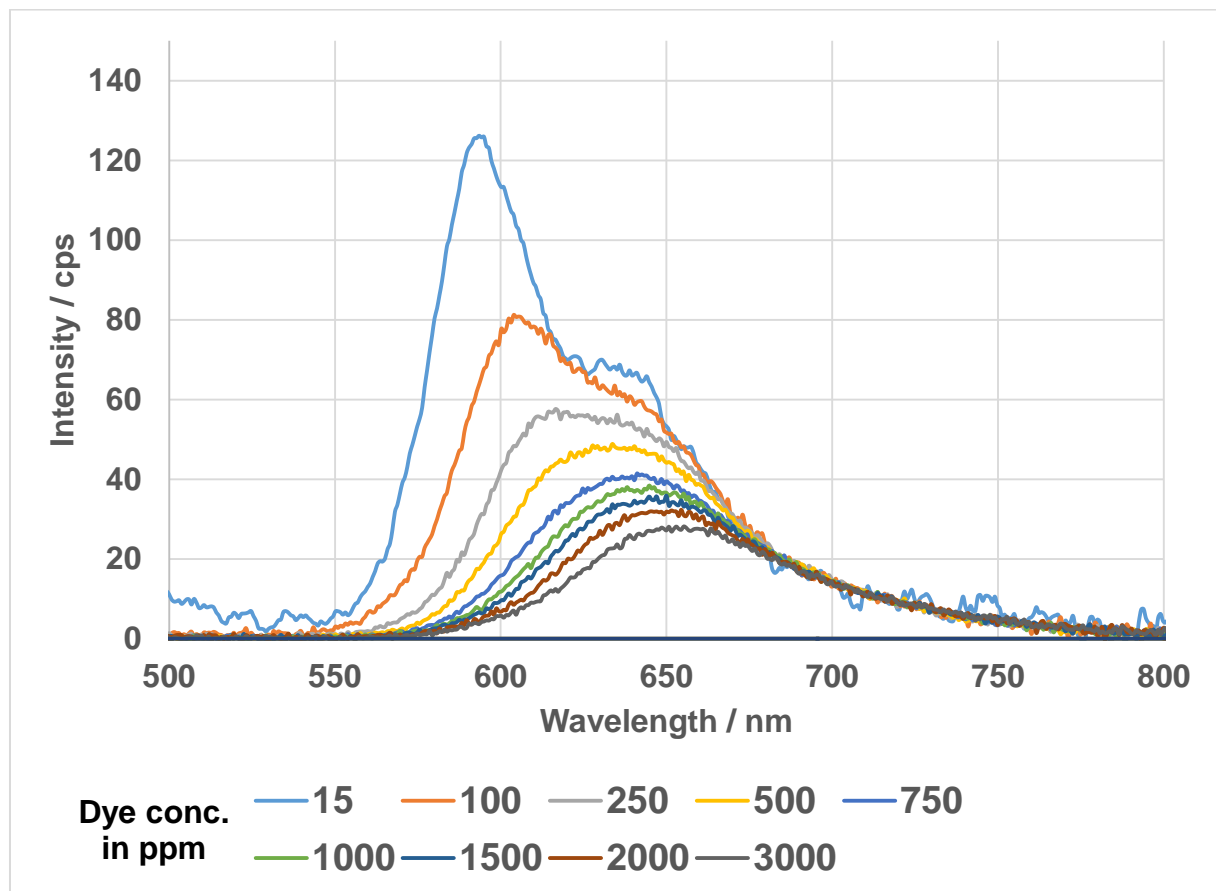


Figure 21. Fitted emission spectra of the Shin(1)FC546 concentration series quantum yield measurement and for the quantum yield correction and self-absorption coefficient calculations.

Table 7. Measured quantum yield values and calculated values of the Shin(1)FC546 concentration series corrected quantum yield and the self-absorption coefficient. Goodness of the fit is calculated and given by the pearsons chi-squared test value χ^2 .

c / ppm	QE	QEcorr	a	χ^2
100	0,93	0,95	0,24	62,22
250	0,73	0,83	0,42	64,12
500	0,65	0,79	0,51	62,39
750	0,56	0,75	0,59	59,64
1000	0,51	0,74	0,62	55,43
1500	0,48	0,72	0,64	53,50
2000	0,42	0,69	0,67	55,03
3000	0,37	0,67	0,71	50,58

Shin(1)FC546 48 h, 200 °C

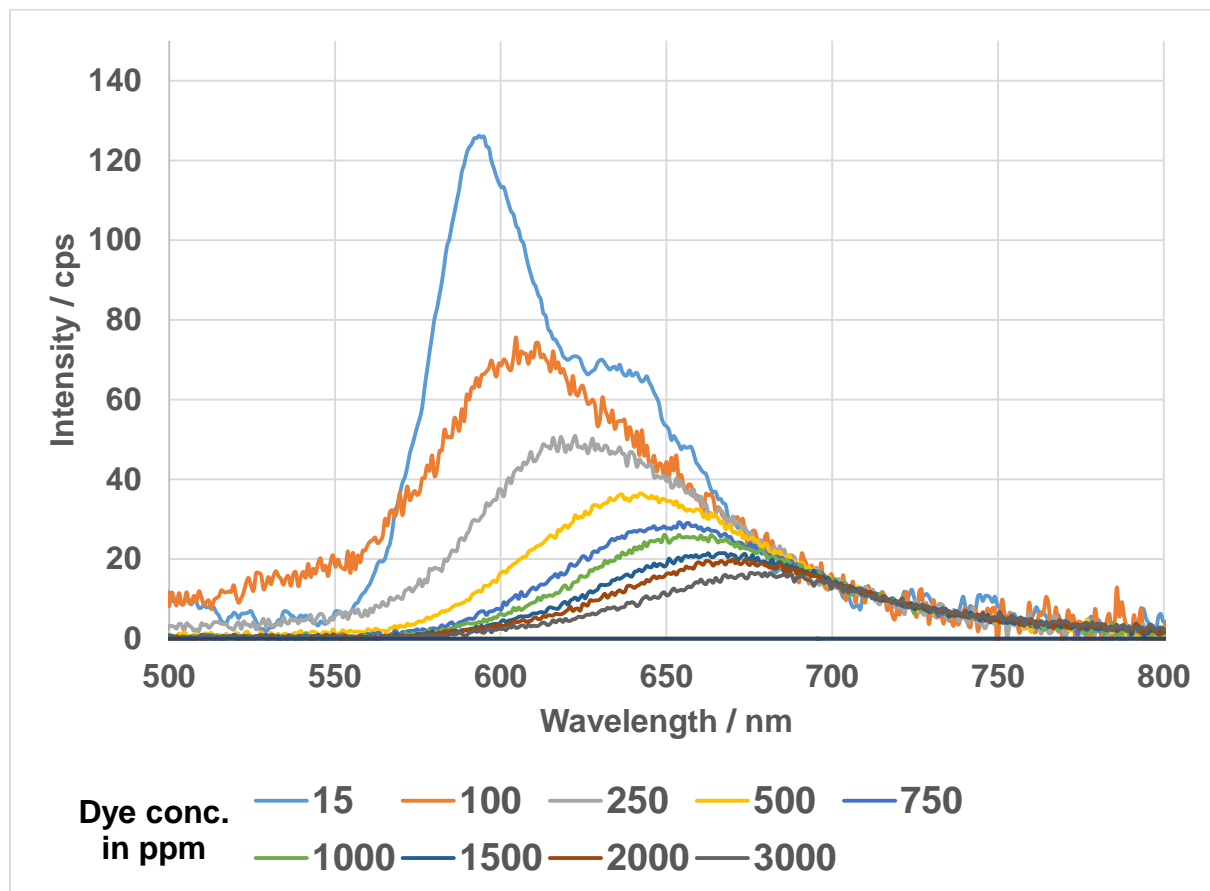


Figure 22. Fitted emission spectra of the Shin(1)FC546 48 h, 200 °C concentration series quantum yield measurement and for the quantum yield correction and self-absorption coefficient calculations.

Table 8. Measured quantum yield values and calculated values of the Shin(1)FC546 48 h, 200 °C concentration series corrected quantum yield and the self-absorption coefficient. Goodness of the fit is calculated and given by the pearsons chi-squared test value χ^2 .

c / ppm	QE	QEcorr	a	χ^2
100	0,37	0,43	0,20	73,64
250	0,40	0,55	0,44	78,24
500	0,43	0,66	0,60	56,22
750	0,40	0,68	0,69	57,11
1000	0,37	0,68	0,72	54,02
1500	0,34	0,68	0,76	54,39
2000	0,31	0,67	0,78	52,17
3000	0,25	0,64	0,81	50,40

Shin(1)FC564 120 h, 200 °C

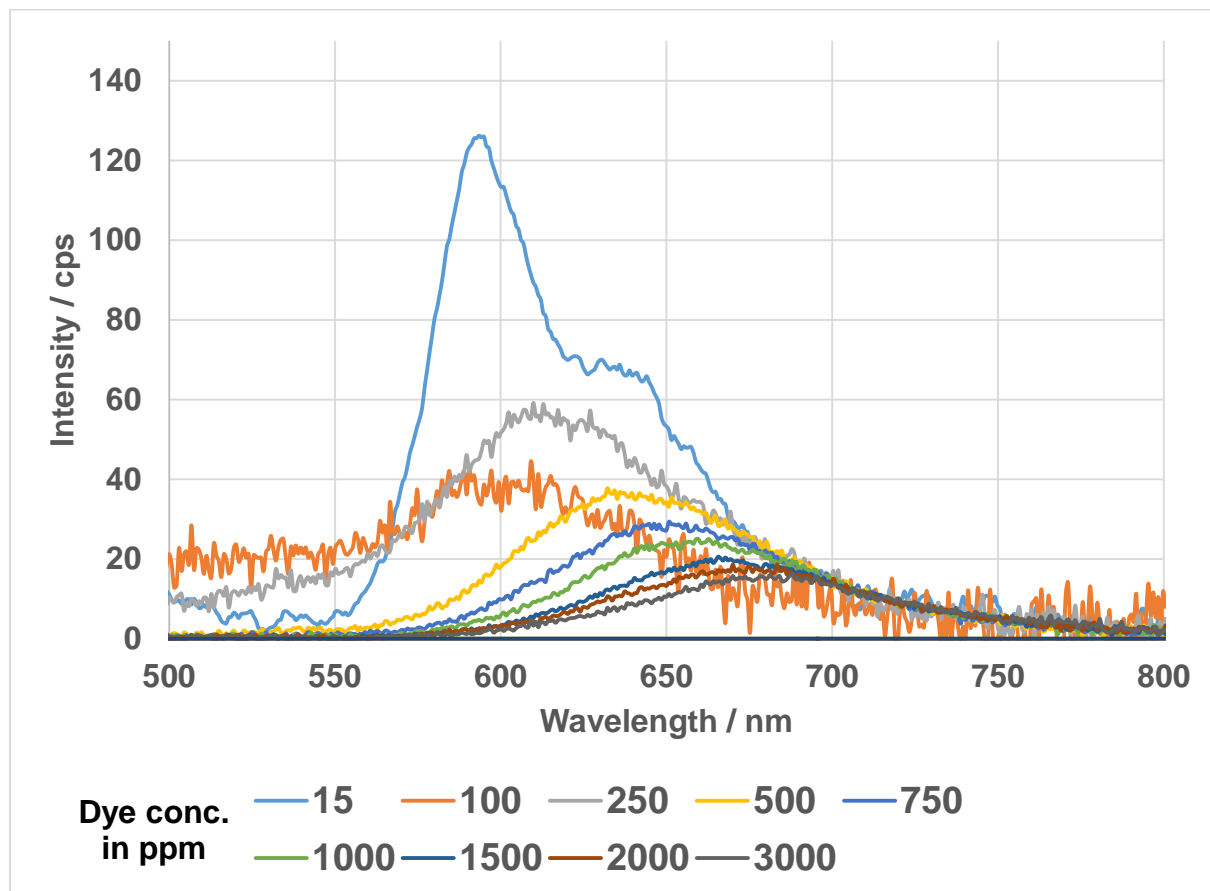


Figure 23. Fitted emission spectra of the Shin(1)FC546 120h, 200 °C concentration series quantum yield measurement and for the quantum yield correction and self-absorption coefficient calculations.

Table 9. Measured quantum yield values and calculated values of the Shin(1)FC546 120h, 200 °C concentration series corrected quantum yield and the self-absorption coefficient. Goodness of the fit is calculated and given by the pearsons chi-squared test value χ^2 .

c / ppm	QE	QEcorr	a	χ^2
100	0,00	0,00	0,49	257,62
250	0,28	0,36	0,32	74,97
500	0,38	0,59	0,58	58,84
750	0,35	0,62	0,68	63,63
1000	0,33	0,64	0,72	52,56
1500	0,30	0,65	0,78	48,48
2000	0,28	0,65	0,79	54,62
3000	0,23	0,62	0,82	45,29

Shin(1)LG305

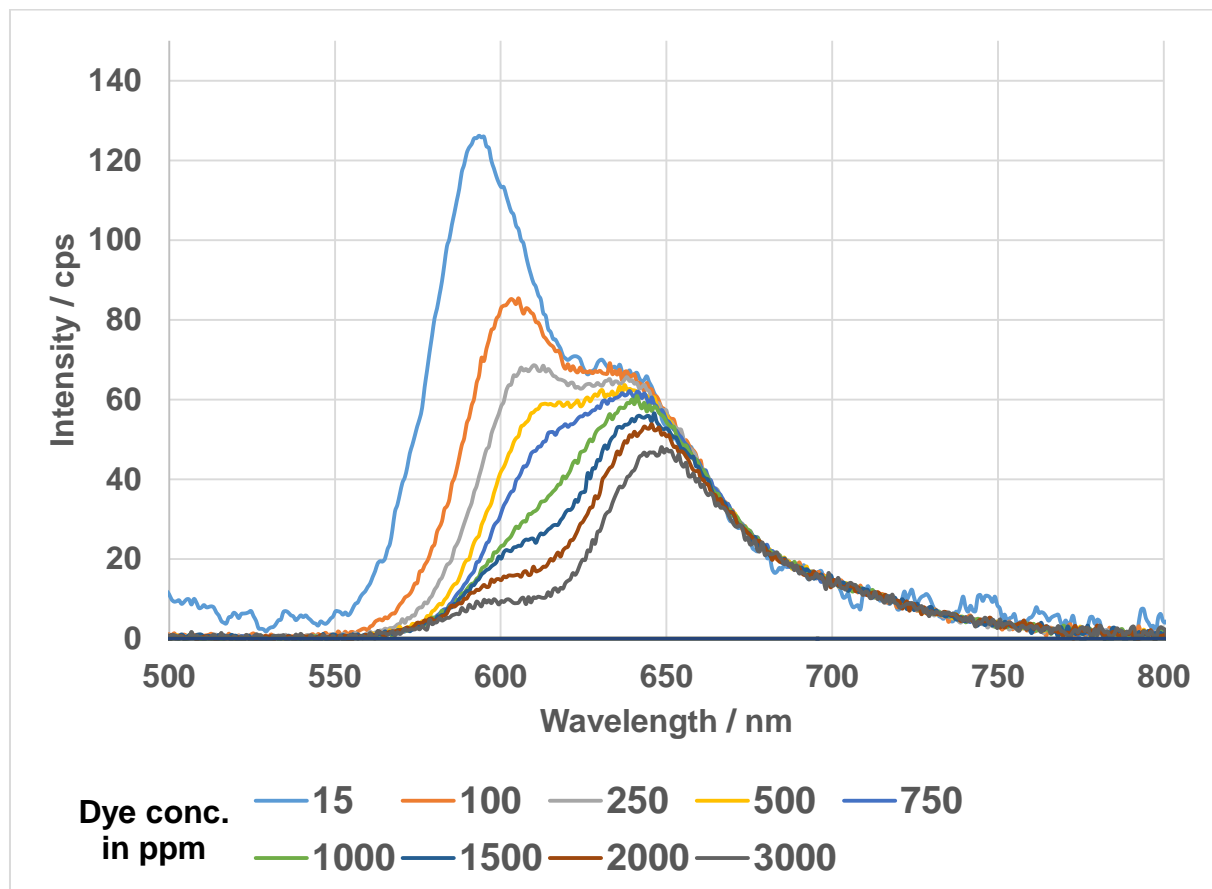


Figure 24. Fitted emission spectra of the Shin(1)LG305 concentration series quantum yield measurement and for the quantum yield correction and self-absorption coefficient calculations.

Table 10. Measured quantum yield values and calculated values of the Shin(1)LG305 concentration series corrected quantum yield and the self-absorption coefficient. Goodness of the fit is calculated and given by the pearsons chi-squared test value χ^2 .

c / ppm	QE	QEcorr	a	χ^2
100	0,90	0,92	0,24	71,81
250	0,92	0,94	0,34	81,92
500	0,91	0,94	0,40	68,63
750	0,85	0,91	0,44	71,71
1000	0,63	0,77	0,49	69,53
1500	0,56	0,73	0,53	73,28
2000	0,38	0,59	0,57	70,53
3000	0,26	0,49	0,63	75,94

Shin(1)LG305 48 h, 200 °C

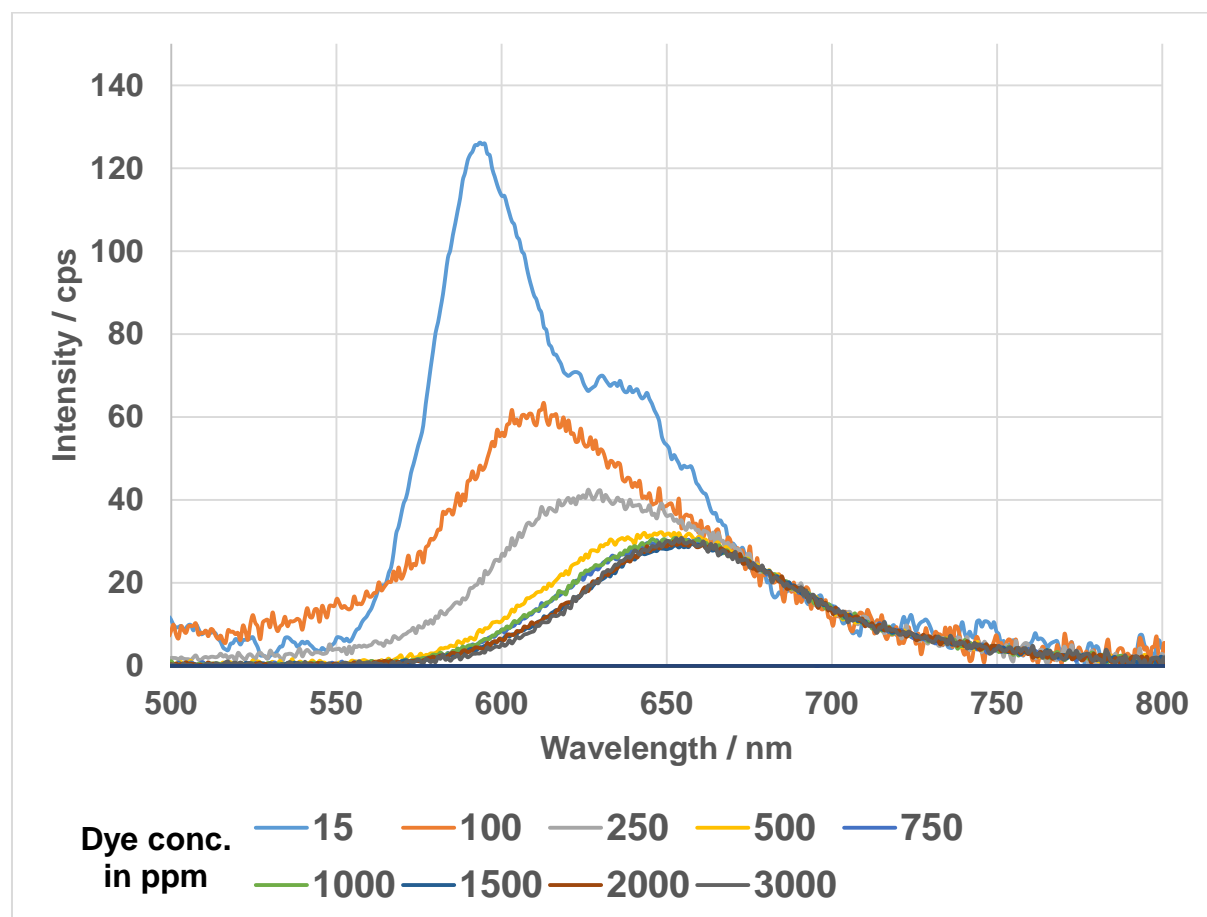


Figure 25. Fitted emission spectra of the Shin(1)LG305 48 h, 200 °C concentration series quantum yield measurement and for the quantum yield correction and self-absorption coefficient calculations.

Table 11. Measured quantum yield values and calculated values of the Shin(1)LG305 48 h, 200 °C concentration series corrected quantum yield and the self-absorption coefficient. Goodness of the fit is calculated and given by the pearsons chi-squared test value χ^2 .

c / ppm	QE	QEcorr	a	χ^2
100	0,36	0,45	0,32	105,20
250	0,41	0,60	0,53	74,73
500	0,49	0,73	0,65	67,99
750	0,50	0,76	0,68	75,67
1000	0,47	0,74	0,68	72,94
1500	0,44	0,73	0,70	70,49
2000	0,35	0,65	0,70	70,07
3000	0,28	0,57	0,70	74,68

Shin(1)LG305 120 h, 200 °C

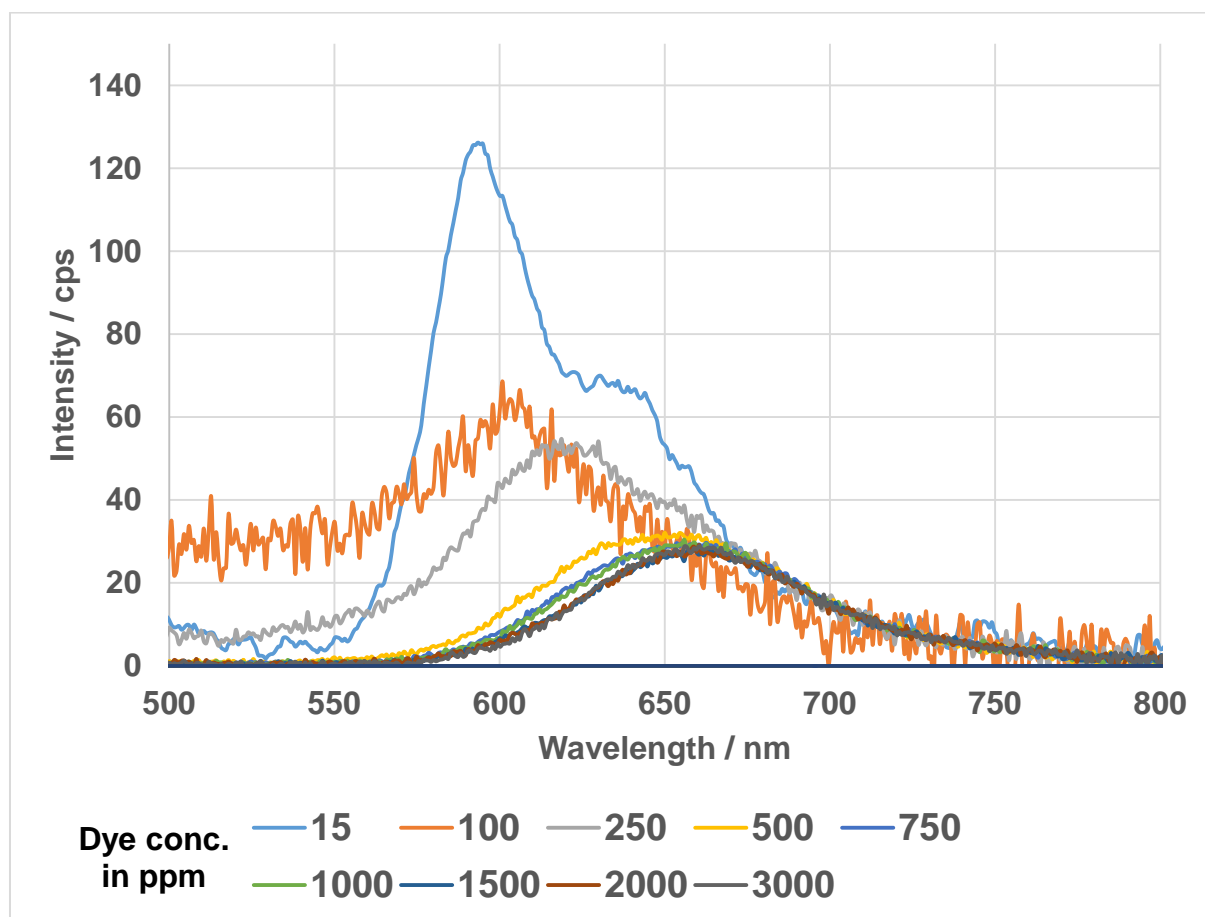


Figure 26. Fitted emission spectra of the Shin(1)LG305 120 h, 200 °C concentration series quantum yield measurement and for the quantum yield correction and self-absorption coefficient calculations.

Table 12. Measured quantum yield values and calculated values of the Shin(1)LG305 120 h, 200 °C concentration series corrected quantum yield and the self-absorption coefficient. Goodness of the fit is calculated and given by the pearsons chi-squared test value χ^2 .

c / ppm	QE	QEcorr	a	χ^2
100	0,21	0,27	0,29	200,40
250	0,28	0,40	0,39	74,72
500	0,39	0,64	0,64	65,11
750	0,40	0,67	0,68	62,49
1000	0,39	0,66	0,68	62,44
1500	0,36	0,66	0,71	63,61
2000	0,28	0,57	0,71	64,90
3000	0,27	0,56	0,71	66,57

Bleaching UV-VIS (Air)

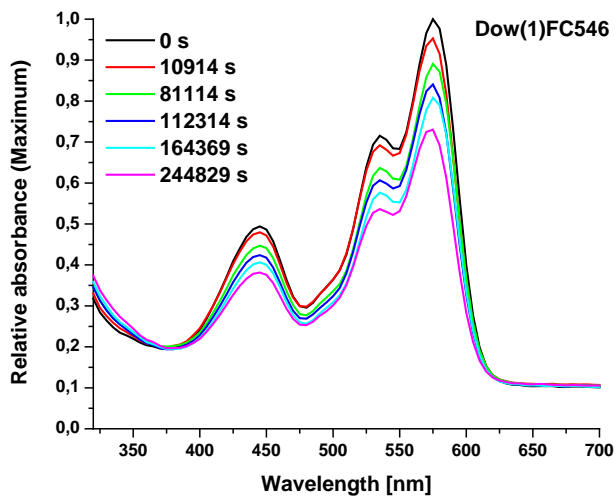


Figure 27. Relative absorbance relevant to the absorbance maximum at 0 s of light exposure and after given time of exposure to 850 mW/cm^{-1} at 450 nm wavelength under Air of the Dow(1)FC546 – 100 ppm sample.

Table 13. Absorbance and relative absorbance relevant to the absorbance at 450 nm at 0 s of light exposure and after given time of exposure to 850 mW/cm^{-1} at 450 nm wavelength under Air of the Dow(1)FC546 – 100 ppm sample.

t / sec	t/ min	Absorbance (450 nm)	Relative absorbance (450 nm)
0	0	0.22951	1
10914	181.9	0.22272	0.97044
81114	1351.9	0.20808	0.90665
112314	1871.9	0.19708	0.85871
164369	2,739	0.18886	0.82291
244829	4,080	0.17731	0.77257

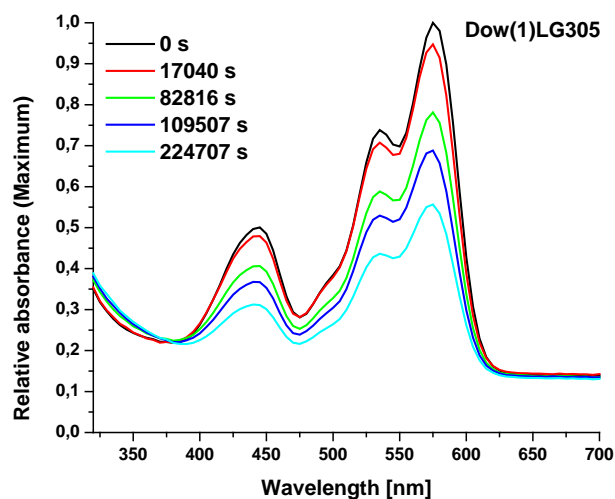


Figure 28. Relative absorbance relevant to the absorbance maximum at 0 s of light exposure and after given time of exposure to 850 mW/cm^{-1} at 450 nm wavelength under Air of the Dow(1)LG305 – 100 ppm sample.

Table 14. Absorbance and relative absorbance relevant to the absorbance at 450 nm at 0 s of light exposure and after given time of exposure to 850 mW/cm^{-1} at 450 nm wavelength under Air of the Dow(1)LG305 – 100 ppm sample.

t / sec	t/ min	Absorbance (450 nm)	Relative absorbance (450 nm)
0	0	0.26795	1
17040	284	0.25597	0.9553
82816	1380.26667	0.21707	0.81012
109507	1825.11667	0.19511	0.72815
224707	3,745	0.16628	0.62055

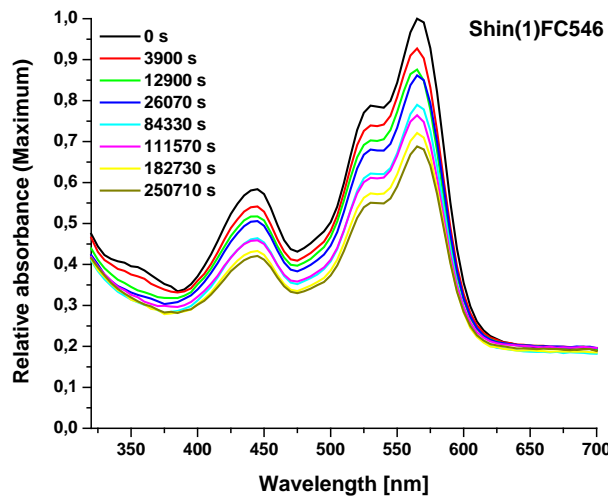


Figure 29. Relative absorbance relevant to the absorbance maximum at 0 s of light exposure and after given time of exposure to 850 mW/cm^{-1} at 450 nm wavelength under Air of the Shin(1)FC546 – 100 ppm sample.

Table 15. Absorbance and relative absorbance relevant to the absorbance at 450 nm at 0 s of light exposure and after given time of exposure to 850 mW/cm^{-1} at 450 nm wavelength under Air of the Shin(1)FC546 – 100 ppm sample.

t / sec	t/ min	Absorbance (450 nm)	Relative absorbance (450 nm)
0	0	0.1732	1
3900	65	0.16022	0.92503
12900	215	0.15374	0.88761
26070	434.5	0.14972	0.86439
84330	1,406	0.13743	0.79345
111570	1,860	0.13632	0.78703
182730	3045.5	0.12833	0.74093
250710	4178.5	0.1247	0.71997

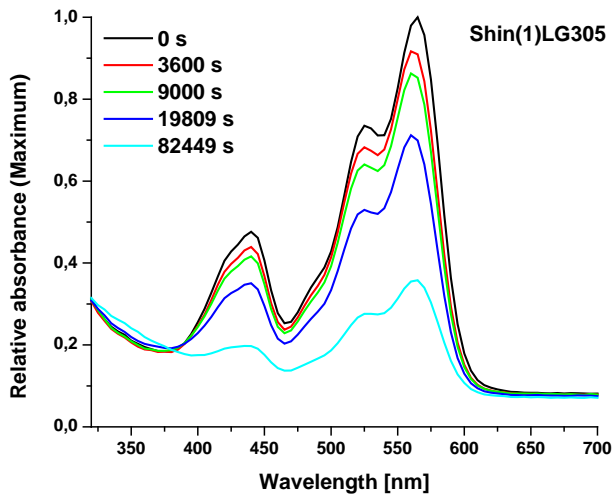


Figure 30. Relative absorbance relevant to the absorbance maximum at 0 s of light exposure and after given time of exposure to 850 mW/cm^{-1} at 450 nm wavelength under Air of the Shin(1)LG305 – 100 ppm sample.

Table 16. Absorbance and relative absorbance relevant to the absorbance at 450 nm at 0 s of light exposure and after given time of exposure to 850 mW/cm^{-1} at 450 nm wavelength under Air of the Shin(1)LG305 – 100 ppm sample.

t / sec	t/ min	Absorbance (450 nm)	Relative absorbance (450 nm)
0	0	0.19157	1
3600	60	0.17353	0.9058
9000	150	0.16436	0.85793
19809	330.15	0.13931	0.72722
82449	1,374	0.08297	0.43312

Bleaching UV-VIS (Nitrogen/Air)

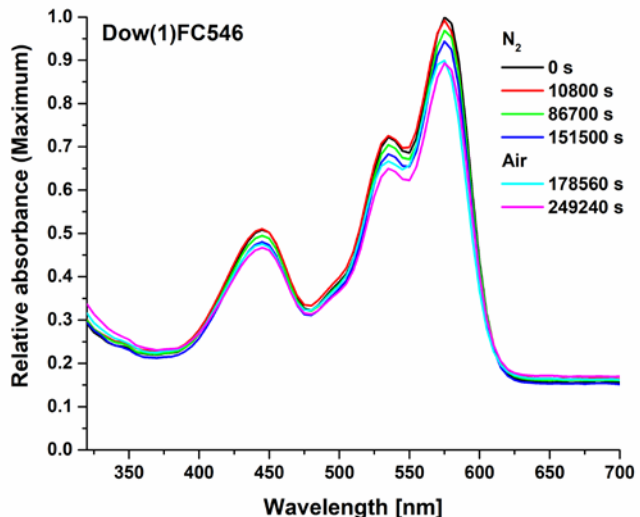


Figure 31. Relative absorbance relevant to the absorbance maximum at 0 s of light exposure and after given time of exposure to 850 mW/cm^{-1} at 450 nm wavelength under Nitrogen/Air of the Dow(1)FC546 – 100 ppm sample.

Table 17. Absorbance and relative absorbance relevant to the absorbance at 450 nm at 0 s of light exposure and after given time of exposure to 850 mW/cm^{-1} at 450 nm wavelength under Nitrogen/Air of the Dow(1)FC546 – 100 ppm sample.

t / sec	t/ min	Absorbance (450 nm)	Relative absorbance (450 nm)
0	0	0.2317	1
10800	180	0.23156	0.9994
86700	1445	0.2253	0.97235
151500	2525	0.21819	0.94167
178560	2976	0.21584	0.93155
249240	4154	0.2127	0.91796

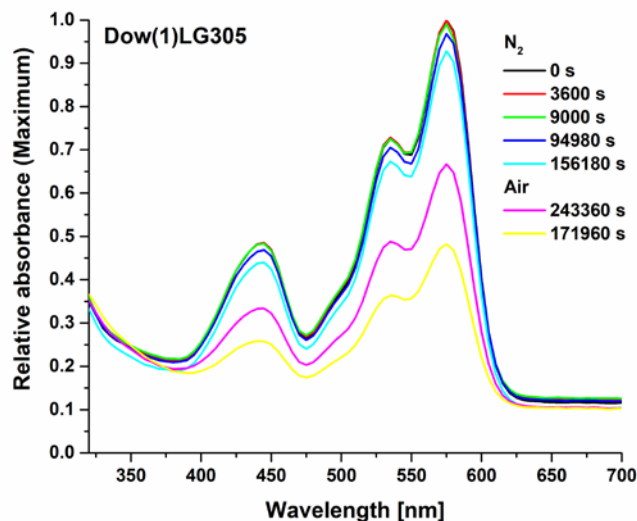


Figure 32. Relative absorbance relevant to the absorbance maximum at 0 s of light exposure and after given time of exposure to 850 mW/cm^{-1} at 450 nm wavelength under Nitrogen/Air of the Dow(1)LG305 – 100 ppm sample.

Table 18. Absorbance and relative absorbance relevant to the absorbance at 450 nm at 0 s of light exposure and after given time of exposure to 850 mW/cm^{-1} at 450 nm wavelength under Nitrogen/Air of the Dow(1)LG305 – 100 ppm sample.

t / sec	t/ min	Absorbance (450 nm)	Relative absorbance (450 nm)
0	0	0.23854	1
3600	60	0.23697	0.99344
9600	160	0.23837	0.99928
94980	1583	0.23092	0.96805
156180	2603	0.21563	0.90396
243360	4056	0.16375	0.68648

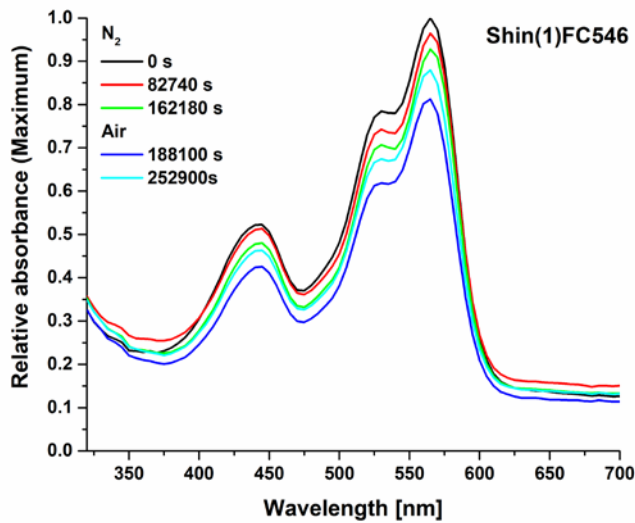


Figure 33. Relative absorbance relevant to the absorbance maximum at 0 s of light exposure and after given time of exposure to 850 mW/cm^2 at 450 nm wavelength under Nitrogen/Air of the Shin(1)FC546 – 100 ppm sample.

Table 19. Absorbance and relative absorbance relevant to the absorbance at 450 nm at 0 s of light exposure and after given time of exposure to 850 mW/cm^2 at 450 nm wavelength under Nitrogen/Air of the Shin(1)FC546 – 100 ppm sample.

t / sec	t/ min	Absorbance (450 nm)	Relative absorbance (450 nm)
0	0	0.15765	1
6900	115	0.14075	0.89279
68100	1135	0.12719	0.80678
153060	2551	0.12749	0.80868
214560	3576	0.11406	0.72348

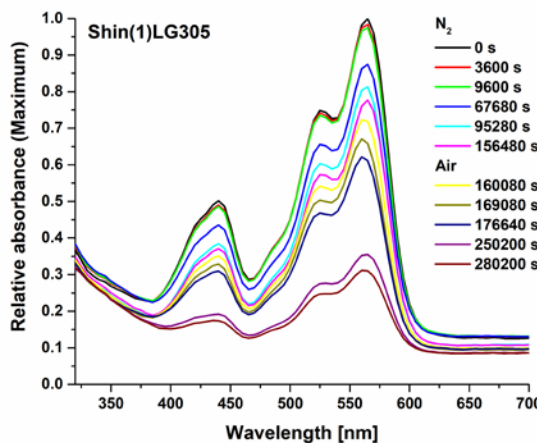


Figure 34. Relative absorbance relevant to the absorbance maximum at 0 s of light exposure and after given time of exposure to 850 mW/cm^2 at 450 nm wavelength under Nitrogen/Air of the Shin(1)LG305 – 100 ppm sample.

Table 20. Absorbance and relative absorbance relevant to the absorbance at 450 nm at 0 s of light exposure and after given time of exposure to 850 mW/cm⁻¹ at 450 nm wavelength under Nitrogen/Air of the Shin(1)LG305 – 100 ppm sample.

t / sec	t/ min	Absorbance (450 nm)	Relative absorbance (450 nm)
0	0	0.21178	1
3600	60	0.20601	0.97279
9600	160	0.20439	0.96511
67680	1128	0.18503	0.87372
95280	1588	0.17142	0.80944
156480	2608	0.16881	0.79712
160080	2668	0.14681	0.69322
169080	2818	0.13679	0.64592
176640	2944	0.12968	0.61235
250200	4170	0.08419	0.39752

Verification of covalent bond formation between a Si-H containing polymer and FC546

In presence of a platinum based hydrosilylation catalyst a reaction between the allyl functionalized FC546 dye and the hydrid groups of Shin Etsu KJR9022E component B under curing conditions should lead to a cured polymer. This polymer should not show any precipitation or any Si-H vibrational Bands in the FTIR spectrum. If there is no bond-formation the dye should precipitate and Si-H vibrations should be present.

Shin Etsu KJR9022E component B (0.1 g) was mixed with a stock solution of FC546 (5.0 g [0.1 wt% in Toluol]; 5 mg FC546) and Platin- Carbonylcyclovinylmethylsiloxan (Ossko-Catalyst; 0.25 µl [2.0% Pt(0) in Xylene]; 255 µg Pt(0); 50 ppm). The solvent was removed under reduced pressure. The polymer dye mixture and the pure component B, as a reference, were transferred into a compartment drier (150 °C, 4 h). The observed solid red but transparent material and the liquid transparent component B were characterized by FTIR spectroscopy.

After the solvent was removed from the polymer dye mixture FC546 precipitated. The heat treatment leads to a cured transparent red Material. FC546 was solved completely in the matrix structure and reacted with the Si-H groups of the polymer covalent bond formation. This was verified by FTIR spectroscopy. The B component of Shin(1) shows vibration bands due to the silicon hydride bond respectively at 2159 cm^{-1} [$\nu(\text{Si-H})$] and 906 cm^{-1} [$\rho(\text{Si-H})$]. By heating the pure B component at curing conditions this vibrational bands are still present. By adding the FC546 dye and a small amount of hydrosilylation catalyst the vibrational bands disappear. The allyl groups of the dye reacted with the Si-H groups of the polymer.

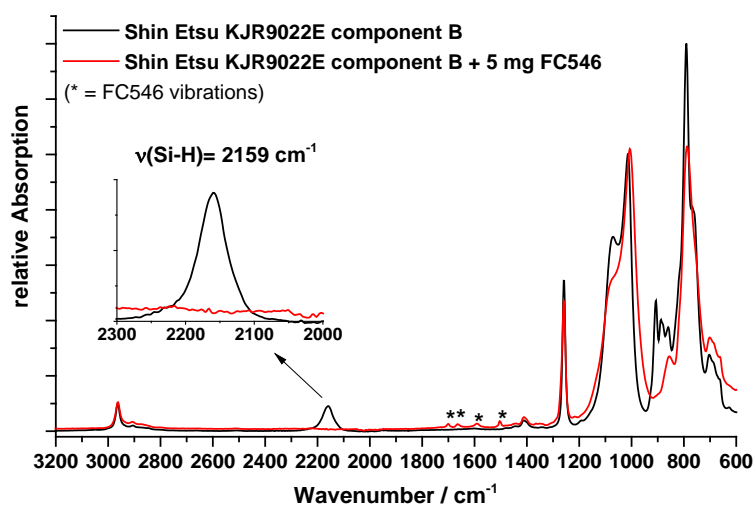


Figure 35. FTIR spectra of pure Shin component B and the dye incorporated component B after heat treatment. The Si-H vibration band disappears completely due to the formation of covalent bonds between the dye and the polymer.